Physics Letters B 797 (2019) 134885

Contents lists available at ScienceDirect

Physics Letters B

www.elsevier.com/locate/physletb

Two-neutrino double electron capture on ^{124}Xe based on an effective theory and the nuclear shell model

E.A. Coello Pérez [a,b,*], J. Menéndez [c], A. Schwenk [a,b,d]

[a] Institut für Kernphysik, Technische Universität Darmstadt, 64289 Darmstadt, Germany
[b] ExtreMe Matter Institute EMMI, Helmholtzzentrum für Schwerionenforschung GmbH, 64291 Darmstadt, Germany
[c] Center for Nuclear Study, The University of Tokyo, Tokyo 113-0033, Japan
[d] Max-Planck-Institut für Kernphysik, Saupfercheckweg 1, 69117 Heidelberg, Germany

ARTICLE INFO

Article history:
Received 22 March 2019
Received in revised form 31 July 2019
Accepted 21 August 2019
Available online 23 August 2019
Editor: J.-P. Blaizot

ABSTRACT

We study the two-neutrino double electron capture on ^{124}Xe based on an effective theory (ET) and large-scale shell model calculations, two modern nuclear structure approaches that have been tested against Gamow-Teller and double-beta decay data. In the ET, the low-energy constants are fit to electron capture and β^- transitions around xenon. For the nuclear shell model, we use an interaction in a large configuration space that reproduces the spectroscopy of nuclei in this mass region. For the dominant transition to the ^{124}Te ground state, we find half-lives $T_{1/2}^{2\nu\mathrm{ECEC}} = (1.3 - 18) \times 10^{22}$ y for the ET and $T_{1/2}^{2\nu\mathrm{ECEC}} = (0.43 - 2.9) \times 10^{22}$ y for the shell model. The ET uncertainty leads to a half-life almost entirely consistent with present experimental limits and largely within the reach of ongoing experiments. The shell model half-life range overlaps with the ET, but extends less beyond current limits. Our findings thus suggest that the two-neutrino double electron capture on ^{124}Xe has a good chance to be discovered by ongoing or future experiments. In addition, we present results for the two-neutrino double electron capture to excited states of ^{124}Te.

1. Introduction

Second-order weak processes give rise to extremely rare decay modes of atomic nuclei. They have been observed in about a dozen nuclei with the longest half-lives in the nuclear chart of about $10^{19} - 10^{21}$ years [1]. All these are two-neutrino double beta ($\beta\beta$) decays, where the emission of two electrons is accompanied by two antineutrinos. An even rarer decay can occur if no neutrinos are emitted, the neutrinoless $\beta\beta$ decay. This process is particularly intriguing, because neutrinoless $\beta\beta$ decay is not allowed in the Standard Model, does not conserve lepton number, and can only happen if neutrinos are their own antiparticles (Majorana particles) [2,3].

Due to its unique potential for neutrino physics, beyond the Standard Model physics, and the understanding of the matter-antimatter asymmetry of the Universe, neutrinoless $\beta\beta$ decay searches are increasingly active [4–10]. The planning and interpretation of these experiments relies on a good understanding of the decay half-life, which depends on a nuclear matrix element. However, these are poorly known as neutrinoless $\beta\beta$ decay matrix-element calculations disagree by at least a factor two [11].

Second-order weak processes with neutrino emission are ideal tests of neutrinoless $\beta\beta$ decay matrix-element calculations. The initial and final states are common, and the transition operator is also very similar, dominated by the physics of spin and isospin. In addition to $\beta\beta$ decay, a related mode is the two-neutrino double electron capture (2νECEC). Here, two K- or L-shell orbital electrons are simultaneously captured, rather than β emitted. This mode is kinematically unfavored with respect to $\beta\beta$ decay, and at present only a geochemical measurement of ^{130}Ba [12,13], and a possible detection in ^{78}Kr [14,15] have been claimed. Moreover, a resonant neutrinoless ECEC could be fulfilled in selected nuclei [16–18]. For both ECEC modes limits of $10^{21} - 10^{22}$ years have been set in various isotopes [12,19–24].

^{124}Xe is one of the most promising isotopes to observe 2νECEC due to its largest Q-value of 2857 keV [25]. Large-volume liquid-xenon experiments primarily designed for the direct detection of dark matter such as XMASS [26], XENON100 [27], or LUX [28] are

* Corresponding author.
E-mail addresses: tcoello@theorie.ikp.physik.tu-darmstadt.de (E.A. Coello Pérez), menendez@cns.s.u-tokyo.ac.jp (J. Menéndez), schwenk@physik.tu-darmstadt.de (A. Schwenk).

https://doi.org/10.1016/j.physletb.2019.134885

sensitive to ECEC and $\beta\beta$ decays in ^{124}Xe, ^{126}Xe and ^{134}Xe [29,30]. Enriched xenon gas detectors are also very competitive [31,32]. Recent searches have reached a sensitivity comparable to the half-lives expected by most theoretical calculations [33,34], a condition only paralleled in ^{78}Kr [14]. Moreover the latest limits set by the XMASS collaboration [35] exclude most theoretical predictions.

Calculations of 2νECEC and two-neutrino $\beta\beta$ decay are challenging because they involve the quantum many-body problem of heavy nuclei with even-even and odd-odd numbers of neutrons and protons. The methods of choice are the quasiparticle random-phase approximation (QRPA) [36,37], extensively used for ^{124}Xe 2νECEC [38–40], and the large-scale nuclear shell model (NSM) [41], which predicted successfully the ^{48}Ca $\beta\beta$ half-live before its measurement [42,43]. In this mass region, shell model studies reproduce well the $\beta\beta$ half-lives of ^{128,130}Te and ^{136}Xe [44–47] and offer a prediction for ^{124}Sn [48]. However no shell-model calculation exists for ^{124}Xe 2νECEC. In addition to QRPA, the interacting boson model [49] and other more schematic approaches have also been applied to ^{124}Xe [50–53].

Further state-of-the-art ^{124}Xe 2νECEC calculations are thus required given the tension between theoretical predictions and experimental limits. In this Letter, we calculate the corresponding nuclear matrix elements using an effective theory (ET), introduced in Ref. [54], which describes well Gamow-Teller and two-neutrino $\beta\beta$ decays of heavy nuclei, including ^{128,130}Te. One of the advantages of the ET is to provide consistent theoretical uncertainties. Similar ETs have been used to study electromagnetic transitions in spherical [55,56] and deformed [57–63] nuclei. In addition, we present the first large-scale nuclear shell model calculation for ^{124}Xe 2νECEC. We focus on transitions to the ^{124}Te $0^+_{\rm gs}$ ground state, but also consider 2νECEC to the lowest excited 0^+_2 and 2^+_1 states. The relation between the calculated nuclear matrix element $M^{2\nu\rm ECEC}$ and the 2νECEC half-life is given by

$$\left(T_{1/2}^{2\nu\rm ECEC}\right)^{-1} = G^{2\nu\rm ECEC} g_A^4 \left|M^{2\nu\rm ECEC}\right|^2 , \tag{1}$$

where $G^{2\nu\rm ECEC}$ is a known phase-space factor [64] and $g_A = 1.27$ the axial-vector coupling constant.

2. Effective theory

We use an ET that describes the initial ^{124}Xe and final ^{124}Te nuclei, both with even number of protons and neutrons, as spherical collective cores. The intermediate nucleus, ^{124}I, has odd number of protons and neutrons. The ET describes its lowest 1^+_1 state as a double-fermion excitation of a 0^+ reference state that represents the ground state of either ^{124}Xe or ^{124}Te, $|1^+_1; j_p; j_n\rangle = \left(n^\dagger \otimes p^\dagger\right)^{(1)} |0^+\rangle$. Depending on the reference state, $n^\dagger$ ($p^\dagger$) creates a neutron (proton) particle or hole in the single-particle orbital j_n (j_p). At leading order, higher 1^+ states are described as multiphonon excitations, with energies with respect to the reference state $E(1^+_{n+1}) = E(1^+_1) + n\omega$, where ω is the excitation energy and n is the number of phonon excitations.

The effective spin-isospin ($\boldsymbol{\sigma\tau}$) Gamow-Teller operator is systematically constructed as the most general rank-one operator. At leading order it takes the form [54]

$$\begin{aligned} O_{\rm GT} = &\, C_\beta \left(\tilde{p} \otimes \tilde{n}\right)^{(1)} \\ &+ \sum_\ell C_{\beta\ell} \left[\left(d^\dagger + \tilde{d}\right) \otimes \left(\tilde{p} \otimes \tilde{n}\right)^{(\ell)}\right]^{(1)} \\ &+ \sum_{L\ell} C_{\beta L\ell} \left[\left(d^\dagger \otimes d^\dagger + \tilde{d} \otimes \tilde{d}\right)^{(L)} \otimes \left(\tilde{p} \otimes \tilde{n}\right)^{(\ell)}\right]^{(1)} \\ &+ \ldots , \end{aligned} \tag{2}$$

where the tilde denotes well defined annihilation tensor operators, and the phonon ($\tilde{d}$, $d^\dagger$) and nucleon operators are tensor coupled. The low-energy constants C must be fitted to data, and the expansion above is truncated after terms involving more than two phonon creation or annihilation operators. The first term in Eq. (2) couples the reference state to the lowest 1^+_1 state of the odd-odd nucleus, so that C_β can be extracted from the known $\log(ft)$ value of the corresponding β decay or EC:

$$C_\beta = \sqrt{\frac{\kappa}{g_A^2 10^{\log(ft)}}} , \tag{3}$$

with dimensionless $\kappa = 6147$ and t in seconds. The power counting of the ET [54–56] relates the Gamow-Teller matrix elements from the lowest and higher 1^+ initial states to the common final reference state by $\langle 0^+|O_{\rm GT}|1^+_{n+1}\rangle \sim (\omega/\Lambda)^{n/2}\langle 0^+|O_{\rm GT}|1^+_1\rangle$, where $\Lambda \sim 3\omega$ is the breakdown scale of the ET. This allows us to estimate the values of $C_{\beta\ell}$ and $C_{L\beta\ell}$ with consistent theoretical uncertainties.

The 2νECEC matrix element from the ground state of the initial nucleus to a 0^+ state of the final one is

$$M^{2\nu\rm ECEC} = \sum_j \frac{\langle 0^+_{\rm f}|O_{\rm GT}|1^+_j\rangle\langle 1^+_j|O_{\rm GT}|0^+_{\rm gs,i}\rangle}{D(1^+_j)/m_e} , \tag{4}$$

where j sums over all 1^+_j states of the intermediate nucleus. The electron mass m_e keeps the matrix element dimensionless, and the energy denominator is $D(1^+_j) = E(1^+_j) - E(0^+_{\rm gs,i}) + [E(0^+_{\rm f}) - E(0^+_{\rm gs,i})]/2$, neglecting the difference in electron binding energies. The expression for the 2νECEC to a final 2^+ state is similar [40], but the energy denominator appears to the third power.

Because the ET is designed to reproduce low-energy states, we calculate the 2νECEC matrix elements within the single-state dominance (SSD) approximation:

$$M^{2\nu\rm ECEC} \approx \frac{\langle 0^+_{\rm f}|O_{\rm GT}|1^+_1\rangle\langle 1^+_1|O^+_{\rm GT}|0^+_{\rm gs,i}\rangle}{D(1^+_1)/m_e} , \tag{5}$$

which implies that only the matrix elements involving the lowest 1^+_1 state contribute. The advantage is that the ET can fit these using Eq. (3). The contribution due to omitted higher intermediate 1^+ states is estimated within the ET and treated as a theoretical uncertainty [54]:

$$\frac{\Delta M^{2\nu\rm ECEC}}{M^{2\nu\rm ECEC}} = \frac{D(1^+_1)}{\Lambda}\Phi\left(\frac{\omega}{\Lambda}, 1, \frac{D(1^+_1)+\omega}{\omega}\right) , \tag{6}$$

where $\Phi(z,s,a) = \sum_{n=0}^\infty z^n/(a+n)^s$ is the Lerch transcendent. The ET describes very well the experimentally known two-neutrino $\beta\beta$ decay half-lives once the ET uncertainties, including from Eq. (6), are taken into account [54]. This agreement includes ^{128,130}Te among other heavy nuclei.

The ET 2νECEC matrix element calculation thus requires the known ground-state energies and the lowest 1^+_1 excitation energy to calculate the energy denominator, as well as the Gamow-Teller β-decay and EC matrix elements from the 1^+_1 to the initial and final states of the 2νECEC to fit the low-energy constants. In addition, the collective mode ω sets the ET uncertainty. Unfortunately, for ^{124}Xe there are no direct measurements for Gamow-Teller β

decay or EC from the lowest 1_1^+ state in ^{124}I (the ground state is 2^-), or alternatively zero-angle charge-exchange reaction cross sections involving the nuclei of interest. The 1_1^+ excitation energy in ^{124}I is also unknown.

Therefore, we adopt the following strategy. First, we set $\log(ft)^{\mathrm{EC}} = 5.00(10)$ for the EC on the lowest 1_1^+ state in ^{124}I, based on the experimental range of known EC on iodine isotopes with nucleon number $A = 122-128$. This quantity varies smoothly for nuclei within an isotopic chain. For the β^- decay, we set $\log(ft)^{\beta^-} = 1.06(1)\log(ft)^{\mathrm{EC}}$, based on the systematics of odd-odd nuclei in this region of the nuclear chart. Guided by the known spin-unassigned excited states of ^{124}I and the systematics in neighboring odd-odd nuclei, we set the excitation energy of the first 1_1^+ state in ^{124}I as $105-170$ keV. Because this range is much smaller than the energy differences in $D(1_1^+)$, the associated uncertainty in the matrix elements is only a few percent. From the above considerations we obtain a range for the ^{124}Xe 2νECEC matrix element based on our choice of parameters entering the ET. Finally, we set the excitation energy to $\omega = 478.3$ keV, the average of the excitation energies of the lowest 2_1^+ states in the corresponding even-even nuclei [54]. This allows us to estimate the ET uncertainty associated to the SSD approximation, Eq. (6).

3. Nuclear shell model

Next we perform large-scale shell model calculations to obtain the nuclear matrix element using the full expression Eq. (4). We solve the many-body Schrödinger equation $H|\psi\rangle = E|\psi\rangle$ for ^{124}Xe, ^{124}Te, ^{124}I, using a shell model Hamiltonian H in the configuration space comprising the $0g_{7/2}$, $1d_{5/2}$, $1d_{3/2}$, $2s_{1/2}$, and $0h_{11/2}$ single-particle orbitals for neutrons and protons. To keep the dimensions of the shell model diagonalization tractable, especially for the largest calculation ^{124}Xe, we need a truncated configuration space. In a first truncation scheme, similar to the one used in Refs. [65,66], we limit to two the number of nucleon excitations from the lower energy $0g_{7/2}$, $1d_{5/2}$ orbitals to the higher lying $1d_{3/2}$, $2s_{1/2}$, $0h_{11/2}$ orbitals. Second, we adopt a complementary truncation scheme that keeps a maximum of two neutron excitations but does not limit the proton excitations from lower to higher lying orbitals (a maximum of six nucleon excitations are permitted in ^{124}Xe). This keeps the $0g_{7/2}$ orbital fully occupied. A third scheme with the $1d_{5/2}$ orbital fully occupied gives results within those of the other two truncations.

We use the shell model interaction GCN5082 [67,68], fitted to spectroscopic properties of nuclei in the mass region of ^{124}Xe. The shell model interaction has been tested against experimental data on Gamow-Teller decays and charge-exchange transitions in this region, showing a good description of data with a renormalization, or "quenching", of the $\boldsymbol{\sigma\tau}$ operator $q = 0.57$ [44]. For the two-neutrino $\beta\beta$ decay of ^{128}Te, ^{130}Te, and ^{136}Xe, however, this interaction fits data best after a larger renormalization $q = 0.48$ [44]. An extreme case is the very small $\beta\beta$ ^{136}Xe matrix element, which is only reproduced with $q = 0.42$ [44]. The renormalization of the spin-isospin operator is needed to correct for the approximations made in the many-body calculation, such as unaccounted correlations beyond the configuration space or neglected two-body currents [11,69]. In particular, for xenon, Ref. [45] suggested that a smaller "quenching" is needed when the spin-orbit partners ($0g_{9/2}$ and $0h_{9/2}$) of the considered configuration space are included. A full understanding of the origin of "quenching" would require an ab initio study that is currently possible only for nuclei lighter than xenon [70–73]. Here we follow the strategy of previous shell model $\beta\beta$ decay predictions [42,43] and include the above "quenching" factors phenomenologically to predict the half-life of ^{124}Xe.

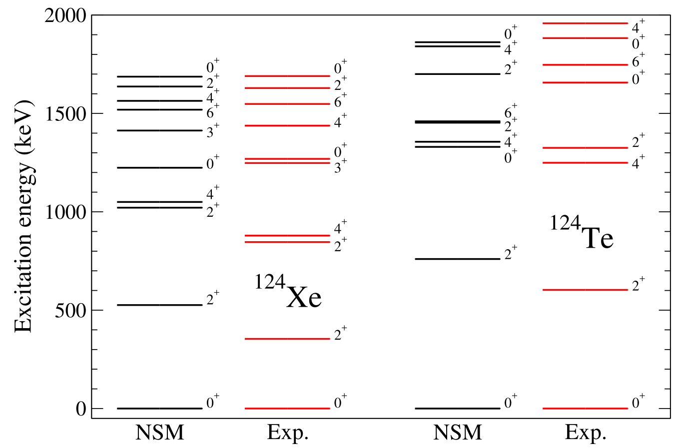

Fig. 1. ^{124}Xe and ^{124}Te excitation spectra obtained by the nuclear shell model (NSM) compared to experiment [74].

The low-energy excitation spectra of the three isotopes are well reproduced. Fig. 1 compares the experimental and calculated spectra for ^{124}Xe and ^{124}Te, obtained with the first truncation scheme described above. The spectra corresponding to the second truncation scheme is of similar quality. When additional excitations to the higher lying orbitals are permitted, the first excited 0_2^+ in ^{124}Te is raised to 1.6 MeV, in much better agreement with experiment. However, such extended truncation yields too large dimensions for ^{124}Xe, and cannot be used in our 2νECEC calculations. The spectra of the intermediate ^{124}I is not well known besides the ground state and few tentative spin assignments. The GCN5082 interaction reproduces correctly the spin and parity of the 2^- ground state, although with a lowest 1_1^+ state at only about 10 keV, below any measured level. For the 2νECEC, as in the ET calculation, we consider the lowest 1_1^+ state at $105-170$ keV excitation energy. All shell model calculations have been performed with the codes ANTOINE and NATHAN [41,75].

4. Results and discussion

The calculated nuclear matrix elements are common for the capture of K- or L-shell electrons. However, the presented half-lives correspond to the ^{124}Xe 2νECEC of two K-shell electrons, as this is the mode explored in recent experiments [31–35].

Table 1 summarizes our main results. The ET predicts a smaller central value for the ^{124}Xe 2νECEC matrix element than the NSM, even though both results are consistent when taking uncertainties into account. The ET uncertainty results from combining the uncertainty associated with the range of the input parameters used for the ET ($\mathrm{ET_{LO}}$ in Table 1) and the uncertainty associated with the SSD approximation, Eq. (6). Both contributions are of similar size. For the NSM, one part of the theoretical uncertainty is given by the range of results obtained with different truncation schemes. The dominant part, however, is given by the three "quenching" values considered: the average $q = 0.57$ and $q = 0.48$, corresponding to the best description of Gamow-Teller transitions and $\beta\beta$ decays, respectively, plus the additional conservative $q = 0.42$ needed in the ^{136}Xe $\beta\beta$ decay. The shell model results in Table 1 cover the two truncations for each of the three "quenching" values (q_1, q_2, q_3). The full NSM result encompasses all these calculations.

Table 1 also shows our predictions for the 2νECEC into excited states of ^{124}Te. For both final 0_2^+ and 2_1^+ states, the ET and NSM matrix elements are consistent, even though the central values predicted by the shell model are about one third of the ET ones. The suppressed NSM matrix element to the final 0_2^+ state

Table 1
Nuclear matrix elements ($M^{2\nu\mathrm{ECEC}}$) and half-lives ($T_{1/2}^{2\nu\mathrm{ECEC}}$) calculated with the ET and the nuclear shell model (NSM). The $\mathrm{ET_{LO}}$ matrix elements do not take into account the uncertainty associated with the SSD approximation, included in the full ET results. The $\mathrm{NSM}_{q_1,q_2,q_3}$ matrix elements assume "quenching" values $q = 0.57, 0.48, 0.42$, respectively, all encompassed in the full NSM range. Results are given for the ^{124}Xe 2νECEC of two K-shell electrons into the ^{124}Te ground 0^+_{gs} and excited 0^+_2 and 2^+_1 states. The phase-space factors $G^{2\nu\mathrm{ECEC}}$ in y^{-1} are from Refs. [40, 64].

2νECEC	$0^+_{\mathrm{gs,i}} \to 0^+_{\mathrm{gs,f}}$	$0^+_{\mathrm{gs,i}} \to 0^+_2$	$0^+_{\mathrm{gs,i}} \to 2^+_1$
$G^{2\nu\mathrm{ECEC}}$	1.72×10^{-20}	1.67×10^{-22}	1.38×10^{-23}
		$M^{2\nu\mathrm{ECEC}}$	
ET	$0.011 - 0.041$	$0.002 - 0.050$	$(0.8 - 9.0) \times 10^{-4}$
$\mathrm{ET_{LO}}$	$0.016 - 0.030$	$0.015 - 0.029$	$(2.7 - 5.4) \times 10^{-4}$
NSM	$0.028 - 0.072$	$0.005 - 0.010$	$(1.1 - 2.3) \times 10^{-4}$
NSM_{q_1}	$0.051 - 0.072$	$0.009 - 0.010$	$(1.9 - 2.3) \times 10^{-4}$
NSM_{q_2}	$0.036 - 0.051$	$0.006 - 0.007$	$(1.4 - 1.6) \times 10^{-4}$
NSM_{q_3}	$0.028 - 0.039$	$0.005 - 0.006$	$(1.1 - 1.2) \times 10^{-4}$
		$T_{1/2}^{2\nu\mathrm{ECEC}}$	
	$[10^{22}\mathrm{y}]$	$[10^{25}\mathrm{y}]$	$[10^{30}\mathrm{y}]$
ET	$1.3 - 18$	$0.092 - 57$	$0.034 - 4.3$
NSM	$0.43 - 2.9$	$2.3 - 9.3$	$0.57 - 2.5$

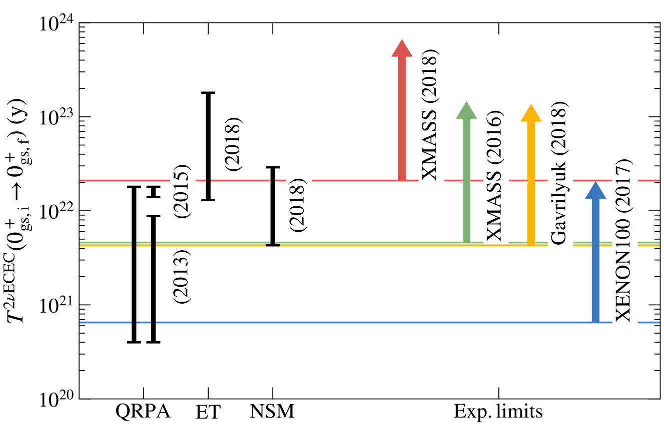

Fig. 2. ^{124}Xe half-life for the 2νECEC of two K-shell electrons. The black bars show the theoretical predictions from the effective theory (ET) and the nuclear shell model (NSM), as well as most recent QRPA calculations [39,40], in comparison to the horizontal lines that indicate the experimental lower limits set by the XENON100 [34] (blue) and XMASS [33,35] (green, red) collaborations as well as Gavrilyuk et al. [32] (yellow).

with respect to the transition to the ground state is consistent with the results on neutrinoless $\beta\beta$ decay in ^{128,130}Te and ^{136}Xe, using the same interaction [67]. While the shell model uncertainties are somewhat smaller than in the 2νECEC to the ground state, the ET ones are much larger, because of the limitations of the SSD approximation when the energy denominator $D(1^+_1)$ is small [54]. The ET and NSM half-lives are in general shorter than the QRPA ones for the 0^+_2 2νECEC [39,40], while for the 2^+_1 2νECEC the NSM and QRPA [40] predictions are very similar. Transitions to excited states are extremely suppressed because of the reduced Q-value and corresponding phase-space factor. The 2νECEC to the final 2^+_1 state, which requires the capture of K- and L-shell electrons, is further suppressed because of the small nuclear matrix element.

Fig. 2 compares our theoretical predictions for the 2νECEC on ^{124}Xe to the ^{124}Te ground state with the most advanced QRPA results from Refs. [39,40] and the most recent experimental 2νECEC limits [32–35]. Theoretical half-lives are shown as black bars. The predictions from the ET, NSM, and QRPA are consistent. However, the ET shows a clear preference for longer half-lives than the NSM. On the other hand, the QRPA spans much shorter half-lives than those predicted by the ET or NSM. The QRPA half-live of Ref. [39] results from two different sets of single-particle energies, quenching values ranging from $q = 0.98 - 0.78$, and energies for the first 1^+ state in ^{124}I between $150 - 1000$ keV. The QRPA half-life of Ref. [40] of the same group employs $q = 0.49$, and we only keep the K-shell 2νECEC. The combined QRPA range is also shown in Fig. 2.

Fig. 2 shows that the theoretical predictions are consistent with the lower half-life limits established by the first results of the XMASS [33] and XENON100 [34] collaborations and with Ref. [32], shown as green, blue and yellow horizontal lines in Fig. 2, respectively. However, the most recent limit established very recently by XMASS [35] (red line) excludes most of our NSM results, but a part of the predicted range remains permitted. Note that since the shell model configuration space had to be truncated, we could not obtain the exact nuclear matrix element without "quenching". On the other hand, the ET half-life is almost fully consistent with the current XMASS limit. The ET central half-life is only about five times longer, and the range predicted by the ET lies largely within the sensitivity of ongoing experiments [34]. The QRPA predictions are mostly excluded including error bars, except the very recent results from Ref. [40], just at the border of the permitted region. Note, however, that assuming a larger "quenching" (at a cost of deteriorating the agreement with β decay data [40]) would lead to a longer QRPA half-life prediction. Most other older theoretical calculations are also in tension with the XMASS limit [35]. Overall, our results suggest that the ^{124}Xe 2νECEC could very well be discovered in ongoing or upcoming experiments in the near future.

5. Summary

We have calculated the nuclear matrix elements for the 2νECEC on ^{124}Xe using an ET and the large-scale nuclear shell model, two of the nuclear many-body approaches best suited to describe β and EC transitions in heavy nuclei. The ET results are based on β decay and EC on neighboring nuclei, while the shell model uses an interaction that describes well $\beta\beta$ decays of neighboring nuclei. The ET provides consistent theoretical uncertainties set by the order of the ET calculation, while the shell model uncertainty is dominated by the range of "quenching" considered for the 2νECEC operator. The ET predicts a half-life consistent and up to several times longer than current experimental limits, while the shell model prediction extends less beyond current limits. When all uncertainties are taken into account, the ET and NSM results are consistent, as well as with the most advanced QRPA results.

Future directions include higher-order calculations in the ET to reduce the uncertainties, and improved NSM studies with a better understanding of the "quenching" of the operator, and limiting truncations in the configuration space. Our findings suggest that the ^{124}Xe 2νECEC has a good chance to be discovered by ongoing or future experiments, so that these predictions can be tested by upcoming analyses of ongoing experiments and can further stimulate future searches.

We thank Alex Fieguth and Catharina Brase for useful discussions. This work was supported in part by the Deutsche Forschungsgesellschaft under Grant SFB 1245, the Japanese Society for the Promotion of Science through Grant 18K03639, MEXT as Priority Issue on Post-K Computer (Elucidation of the Fundamental Laws and Evolution of the Universe), JICFus and the CNS-RIKEN joint project for large-scale nuclear structure calculations.

Note added in proof

After submission of our manuscript, the XENON collaboration reported the discovery of the 2νECEC on ^{124}Xe in very good agreement with our ET and NSM predictions [76].

References

[1] A.S. Barabash, Average and recommended half-life values for two-neutrino double beta decay, Nucl. Phys. A 935 (2015) 52.
[2] F.T. Avignone, S.R. Elliott, J. Engel, Double beta decay, Majorana neutrinos, and neutrino mass, Rev. Mod. Phys. 80 (2008) 481.
[3] J.D. Vergados, H. Ejiri, F. Šimkovic, Theory of neutrinoless double-beta decay, Rept. Prog. Phys. 75 (2012) 106301.
[4] A. Gando, et al., KamLAND-Zen Collaboration, Search for Majorana neutrinos near the inverted mass hierarchy region with KamLAND-Zen, Phys. Rev. Lett. 117 (2016) 082503.
[5] J.B. Albert, et al., EXO Collaboration, Search for neutrinoless double-beta decay with the upgraded EXO-200 detector, Phys. Rev. Lett. 120 (2018) 072701.
[6] C. Alduino, et al., CUORE Collaboration, First results from CUORE: a search for lepton number violation via $0\nu\beta\beta$ decay of ^{130}Te, Phys. Rev. Lett. 120 (2018) 132501.
[7] C.E. Aalseth, et al., Majorana Collaboration, Search for neutrinoless double-β decay in ^{76}Ge with the Majorana demonstrator, Phys. Rev. Lett. 120 (2018) 132502.
[8] M. Agostini, et al., GERDA Collaboration, Improved limit on neutrinoless double-β decay of ^{76}Ge from GERDA phase II, Phys. Rev. Lett. 120 (2018) 132503.
[9] A.D. McDonald, et al., NEXT Collaboration, Demonstration of single barium ion sensitivity for neutrinoless double beta decay using single molecule fluorescence imaging, Phys. Rev. Lett. 120 (2018) 132504.
[10] O. Azzolini, et al., CUPID-0 Collaboration, First result on the neutrinoless double-β decay of ^{82}Se with CUPID-0, Phys. Rev. Lett. 120 (2018) 232502.
[11] J. Engel, J. Menéndez, Status and future of nuclear matrix elements for neutrinoless double-beta decay: a review, Rept. Prog. Phys. 80 (2017) 046301.
[12] A.P. Meshik, C.M. Hohenberg, O.V. Pravdivtseva, Ya.S. Kapusta, Weak decay of ^{130}Ba and ^{132}Ba: geochemical measurements, Phys. Rev. C 64 (2001) 035205.
[13] M. Pujol, B. Marty, P. Burnard, P. Philippot, Xenon in archean barite: weak decay of ^{130}Ba, mass-dependent isotopic fractionation and implication for barite formation, Geochim. Cosmochim. Acta 73 (2009) 6834.
[14] Yu.M. Gavrilyuk, A.M. Gangapshev, V.V. Kazalov, V.V. Kuzminov, S.I. Panasenko, S.S. Ratkevich, Indications of $2\nu 2K$ capture in ^{78}Kr, Phys. Rev. C 87 (2013) 035501.
[15] S.S. Ratkevich, A.M. Gangapshev, Yu.M. Gavrilyuk, F.F. Karpeshin, V.V. Kazalov, V.V. Kuzminov, S.I. Panasenko, M.B. Trzhaskovskaya, S.P. Yakimenko, Comparative study of the double K-shell-vacancy production in single- and double-electron capture decay, Phys. Rev. C 96 (2017) 065502.
[16] M.I. Krivoruchenko, F. Šimkovic, D. Frekers, A. Faessler, Resonance enhancement of neutrinoless double electron capture, Nucl. Phys. A 859 (2011) 140.
[17] S. Eliseev, et al., Resonant enhancement of neutrinoless double-electron capture in ^{152}Gd, Phys. Rev. Lett. 106 (2011) 052504.
[18] S. Eliseev, et al., Multiple-resonance phenomenon in neutrinoless double-electron capture, Phys. Rev. C 84 (2011) 012501.
[19] G. Angloher, M. Bauer, P. Bauer, I. Bavykina, A. Bento, C. Bucci, L. Canonica, C. Ciemniak, X. Defay, G. Deuter, et al., New limits on double electron capture of ^{40}Ca and ^{180}W, J. Phys. G 43 (2016) 095202.
[20] B. Lehnert, D. Degering, A. Frotscher, T. Michel, K. Zuber, A search for the radiative neutrinoless double-electron capture of ^{58}Ni, J. Phys. G 43 (2016) 065201.
[21] M. Agostini, et al., GERDA, Limit on the radiative neutrinoless double electron capture of ^{36}Ar from GERDA phase I, Eur. Phys. J. C 76 (2016) 652.
[22] A.S. Barabash, Ph. Hubert, Ch. Marquet, A. Nachab, S.I. Konovalov, F. Perrot, F. Piquemal, V. Umatov, Improved limits on β^+EC and ECEC processes in ^{112}Sn, Phys. Rev. C 83 (2011) 045503.
[23] P. Belli, et al., Search for 2β decays of ^{96}Ru and ^{104}Ru by ultralow-background HPGe γ spectrometry at LNGS: final results, Phys. Rev. C 87 (2013) 034607.
[24] P. Belli, et al., Search for 2β decay of ^{106}Cd with an enriched $^{106}CdWO_4$ crystal scintillator in coincidence with four HPGe detectors, Phys. Rev. C 93 (2016) 045502.
[25] D.A. Nesterenko, et al., Double-beta transformations in isobaric triplets with mass numbers $A = 124$, 130, and 136, Phys. Rev. C 86 (2012) 044313.
[26] K. Abe, K. Hieda, K. Hiraide, S. Hirano, Y. Kishimoto, K. Kobayashi, S. Moriyama, K. Nakagawa, M. Nakahata, H. Nishiie, et al., XMASS detector, Nucl. Instrum. Methods Phys. Res. A 716 (2013) 78.
[27] E. Aprile, et al., XENON100 Collaboration, The XENON100 dark matter experiment, Astropart. Phys. 35 (2012) 573.
[28] D.S. Akerib, et al., LUX Collaboration, First results from the LUX dark matter experiment at the Sanford Underground Research Facility, Phys. Rev. Lett. 112 (2014) 091303.
[29] D.-M. Mei, I. Marshall, W.-Z. Wei, C. Zhang, Measuring double-electron capture with liquid xenon experiments, Phys. Rev. C 89 (2014) 014608.
[30] N. Barros, J. Thurn, K. Zuber, Double beta decay searches of ^{134}Xe, ^{126}Xe and ^{124}Xe with large scale Xe detectors, J. Phys. G 41 (2014) 115105.
[31] Yu.M. Gavrilyuk, A.M. Gangapshev, V.V. Kazalov, V.V. Kuzminov, S.I. Panasenko, S.S. Ratkevich, D.A. Tekueva, S.P. Yakimenko, Search for $2K(2\nu)$-capture of ^{124}Xe, in: Proceedings, 2nd International Workshop on Prospects of Particle Physics: Neutrino Physics and Astrophysics, Valday, Russia, February 1–8, 2015, Phys. Part. Nucl. 48 (2017) 38.
[32] Yu.M. Gavrilyuk, A.M. Gangapshev, V.V. Kazalov, V.V. Kuzminov, S.I. Panasenko, S.S. Ratkevich, D.A. Tekueva, Search for two-neutrino 2K capture in ^{124}Xe: the method and preliminary results, in: Proceedings, International Session-Conference of the SNP of PSD RAS "Physics of Fundamental Interactions", Dubna, Russia, April 12–15, 2016, Phys. Part. Nucl. 49 (2018) 36.
[33] K. Abe, et al., XMASS Collaboration, Search for two-neutrino double electron capture on ^{124}Xe with the XMASS-I detector, Phys. Lett. B 759 (2016) 64.
[34] E. Aprile, et al., XENON Collaboration, Search for two-neutrino double electron capture of ^{124}Xe with XENON100, Phys. Rev. C 95 (2017) 024605.
[35] K. Abe, et al., XMASS Collaboration, Improved search for two-neutrino double electron capture on ^{124}Xe and ^{126}Xe using particle identification in XMASS-I, Prog. Theor. Exp. Phys. 2018 (2018) 053D03.
[36] J. Suhonen, O. Civitarese, Double-beta-decay nuclear matrix elements in the QRPA framework, J. Phys. G 39 (2012) 085105.
[37] F. Šimkovic, V. Rodin, A. Faessler, P. Vogel, $0\nu\beta\beta$ and $2\nu\beta\beta$ nuclear matrix elements, quasiparticle random-phase approximation, and isospin symmetry restoration, Phys. Rev. C 87 (2013) 045501.
[38] M. Hirsch, K. Muto, T. Oda, H.V. Klapdor-Kleingrothaus, Nuclear structure calculation of $\beta^+\beta^+$, β^+/EC and EC/EC decay matrix elements, Z. Phys. A 347 (1994) 151.
[39] J. Suhonen, Double beta decays of ^{124}Xe investigated in the QRPA framework, J. Phys. G 40 (2013) 075102.
[40] P. Pirinen, J. Suhonen, Systematic approach to β and $2\nu\beta\beta$ decays of mass $A = 100 - 136$ nuclei, Phys. Rev. C 91 (2015) 054309.
[41] E. Caurier, G. Martínez-Pinedo, F. Nowacki, A. Poves, A.P. Zuker, The shell model as unified view of nuclear structure, Rev. Mod. Phys. 77 (2005) 427.
[42] E. Caurier, A.P. Zuker, A. Poves, A full $0\hbar\omega$ description of the $2\nu\beta\beta$ decay of ^{48}Ca, Phys. Lett. B 252 (1990) 13.
[43] A. Poves, R.P. Bahukutumbi, K. Langanke, P. Vogel, Double beta decay of ^{48}Ca revisited, Phys. Lett. B 361 (1995) 1–4.
[44] E. Caurier, F. Nowacki, A. Poves, Shell model description of the $\beta\beta$ decay of ^{136}Xe, Phys. Lett. B 711 (2012) 62.
[45] M. Horoi, B.A. Brown, Shell-model analysis of the ^{136}Xe double beta decay nuclear matrix elements, Phys. Rev. Lett. 110 (2013) 222502.
[46] M. Horoi, A. Neacsu, Shell model predictions for ^{124}Sn double-β decay, Phys. Rev. C 93 (2016) 024308.
[47] L. Coraggio, L. De Angelis, T. Fukui, A. Gargano, N. Itaco, Calculation of Gamow-Teller and two-neutrino double-β decay properties for ^{130}Te and ^{136}Xe with realistic nucleon-nucleon potential, Phys. Rev. C 95 (2017) 064324.
[48] A. Neacsu, M. Horoi, Shell model studies of the ^{130}Te neutrinoless double-beta decay, Phys. Rev. C 91 (2015) 024309.
[49] J. Barea, J. Kotila, F. Iachello, $0\nu\beta\beta$ and $2\nu\beta\beta$ nuclear matrix elements in the interacting boson model with isospin restoration, Phys. Rev. C 91 (2015) 034304.
[50] A. Shukla, P.K. Raina, P.K. Rath, Study of two neutrino $\beta^+\beta^+/\beta^+$EC/ECEC decay of ^{124,126}Xe and ^{130,132}Ba for $0^+ \to 0^+$ transition in PHFB model, J. Phys. G 34 (2007) 549.
[51] S. Singh, R. Chandra, P.K. Rath, P.K. Raina, J.G. Hirsch, Nuclear deformation and the two-neutrino double-β decay in ^{124,126}Xe, ^{128,130}Te, ^{130,132}Ba and ^{150}Nd isotopes, Eur. Phys. J. A 33 (2007) 375.
[52] O.A. Rumyantsev, M.H. Urin, The strength of the analog and Gamow-Teller giant resonances and hindrance of the $2\nu\beta\beta$-decay rate, Phys. Lett. B 443 (1998) 51.
[53] M. Aunola, J. Suhonen, Systematic study of beta and double beta decay to excited final states, Nucl. Phys. A 602 (1996) 133.
[54] E.A. Coello Pérez, J. Menéndez, A. Schwenk, Gamow-Teller and double-beta decays of heavy nuclei within an effective theory, Phys. Rev. C 98 (2018) 045501.
[55] E.A. Coello Pérez, T. Papenbrock, Effective field theory for nuclear vibrations with quantified uncertainties, Phys. Rev. C 92 (2015) 064309.
[56] E.A. Coello Pérez, T. Papenbrock, Effective field theory for vibrations in odd-mass nuclei, Phys. Rev. C 94 (2016) 054316.
[57] T. Papenbrock, Effective theory for deformed nuclei, Nucl. Phys. A 852 (2011) 36.
[58] J. Zhang, T. Papenbrock, Rotational constants of multi-phonon bands in an effective theory for deformed nuclei, Phys. Rev. C 87 (2013) 034323.
[59] T. Papenbrock, H.A. Weidenmüller, Effective field theory for finite systems with spontaneously broken symmetry, Phys. Rev. C 89 (2014) 014334.
[60] E.A. Coello Pérez, T. Papenbrock, Effective theory for the nonrigid rotor in an electromagnetic field: toward accurate and precise calculations of $E2$ transitions in deformed nuclei, Phys. Rev. C 92 (2015) 014323.
[61] T. Papenbrock, H.A. Weidenmüller, Effective field theory of emergent symmetry breaking in deformed atomic nuclei, J. Phys. G 42 (2015) 105103.
[62] Q.B. Chen, N. Kaiser, U.-G. Meißner, J. Meng, Effective field theory for triaxially deformed nuclei, Eur. Phys. J. A 53 (2017) 204.
[63] Q.B. Chen, N. Kaiser, Ulf-G. Meißner, J. Meng, Effective field theory for collective rotations and vibrations of triaxially deformed nuclei, Phys. Rev. C 97 (2018) 064320.
[64] J. Kotila, F. Iachello, Phase space factors for $\beta^+\beta^+$ decay and competing modes of double-β decay, Phys. Rev. C 87 (2013) 024313.

[65] P. Klos, J. Menéndez, D. Gazit, A. Schwenk, Large-scale nuclear structure calculations for spin-dependent WIMP scattering with chiral effective field theory currents, Phys. Rev. D 88 (2013) 083516, Erratum: Phys. Rev. D 89 (2014) 029901.

[66] L. Vietze, P. Klos, J. Menéndez, W.C. Haxton, A. Schwenk, Nuclear structure aspects of spin-independent WIMP scattering off xenon, Phys. Rev. D 91 (2015) 043520.

[67] J. Menéndez, A. Poves, E. Caurier, F. Nowacki, Disassembling the nuclear matrix elements of the neutrinoless $\beta\beta$ decay, Nucl. Phys. A 818 (2009) 139.

[68] E. Caurier, F. Nowacki, A. Poves, K. Sieja, Collectivity in the light xenon isotopes: a shell model study, Phys. Rev. C 82 (2010) 064304.

[69] J. Menéndez, D. Gazit, A. Schwenk, Chiral two-body currents in nuclei: Gamow-Teller transitions and neutrinoless double-beta decay, Phys. Rev. Lett. 107 (2011) 062501.

[70] Doron Gazit, Sofia Quaglioni, Petr Navratil, Three-nucleon low-energy constants from the consistency of interactions and currents in chiral effective field theory, Phys. Rev. Lett. 103 (2009) 102502, Erratum: Phys. Rev. Lett. 122 (2019) 029901.

[71] P. Klos, A. Carbone, K. Hebeler, J. Menéndez, A. Schwenk, Uncertainties in constraining low-energy constants from ^{3}H β decay, Eur. Phys. J. A 53 (2017) 168, Erratum: Eur. Phys. J. A 54 (2018) 76.

[72] A. Ekström, G.R. Jansen, K.A. Wendt, G. Hagen, T. Papenbrock, S. Bacca, B. Carlsson, D. Gazit, Effects of three-nucleon forces and two-body currents on Gamow-Teller strengths, Phys. Rev. Lett. 113 (2014) 262504.

[73] S. Pastore, A. Baroni, J. Carlson, S. Gandolfi, S.C. Pieper, R. Schiavilla, R.B. Wiringa, Quantum Monte Carlo calculations of weak transitions in $A = 6 - 10$ nuclei, Phys. Rev. C 97 (2018) 022501.

[74] http://www.nndc.bnl.gov/ensdf/.

[75] E. Caurier, F. Nowacki, Acta Phys. Pol. B 30 (1999) 705.

[76] E. Aprile, et al., XENON, Observation of two-neutrino double electron capture in ^{124}Xe with XENON1T, Nature 568 (2019) 532.